

The Lorenz number L becomes

$$L(J)/L(0) = 1 + l, \quad (14)$$

where

$$l = \left\{ \sum_{s=1} A(s,y) [E(s,2) - E(s,0)] \right\} / \left[\sum_{s=0} A(s,y) E(s,0) \right],$$

and $L(0) = K(0)/\sigma(0)T$ is the Lorenz number when $J=0$. One can easily calculate $E(s,n)$ directly from Eq. (10), or by using $S(n,m,2r)$ and $U(n,m,2r)$. In the limit $|y| \rightarrow \infty$, the temperature-dependent function $G(s,y)$ goes to zero as $|y|^{-2-s}$. In this limit the Lorenz number becomes

$$L(J)/L(0) = 1 + 0.6666G(1,y) + \dots \quad (15)$$

Here we have used $E(1,2) = 1.0529$ and $E(1,0) = 0.3863$ obtained from Eqs. (5) and (10). Thus we expect that there is a maximum in the Lorenz number at a certain temperature. One can determine a temperature T_m at which l has a maximum l_m by solving

$$\partial l / \partial y = 0.$$

Note that T_m and l_m depend upon only one parameter C_0 . T_m may be less or greater than T_K . By introducing the residual electrical and thermal conductivities, a minimum in the Lorenz number has been discussed by Wilson.³ Suhl and Wong,⁴ using the S -matrix formula-

³ A. H. Wilson, *The Theory of Metals* (Cambridge University Press, New York, 1965), 2nd ed., p. 290.

⁴ H. Suhl and D. Wong, *Physics* **3**, 17 (1967).

tion of the problem of exchange scattering of electrons, carried out a numerical calculation of the Lorenz number, and they found a maximum in L at a certain temperature. Recently, Murata and Wilkins⁵ calculated the Lorenz number numerically by taking into account only exchange scattering for $\text{Im}t(\omega)$; in other words, using $g(x,y)$ in place of $[1 + C_0g(x,y)]$ in Eq. (7). They found that L increases about 40% with temperatures up to $2T_K$ and stays constant at higher temperatures.

Note added in proof. One of us (S. B. Nam in supplement to the New Physics (Sae-Mool-Ri), Seoul, Korea, 1969) has carried out the calculations of transport coefficients for metals, taking into account the scattering of conduction electrons by magnetic impurities of ordinary and exchange (s - d) interactions. The Lorenz number for this case also has a maximum, and the thermoelectric power has a maximum or a minimum depending upon the sign of the potential scattering.

We thank Professor V. Celli, Professor D. Beck, and Professor M. Fowler for discussions. One of us (S. B. N.) thanks Professor Wilkins for sending him the unpublished result of the Lorenz number of Ref. 5.

⁵ J. W. Wilkins (private communication); K. K. Murata and J. W. Wilkins, in *Proceedings of the Eleventh International Conference on Low-Temperature Physics*, edited by J. H. Allen, D. M. Finlayson, and D. M. McCall (University of St. Andrews Printing Department, St. Andrews, Scotland, 1969), p. 1242. They reported numerical results of $K/K_0 \approx \sigma/\sigma_0$.

High-Field Magnetization of Thulium Single Crystals*

D. B. RICHARDS† AND S. LEGVOLD

Institute for Atomic Research and Department of Physics, Iowa State University, Ames, Iowa 50010

(Received 9 May 1969)

The magnetization of thulium has been measured along the $\langle 10\bar{1}0 \rangle$ (b axis) and $\langle 0001 \rangle$ (c axis) directions from 4.2 to 300°K in magnetic fields up to 100 kOe. The measurements were taken using a vibrating-sample magnetometer designed and constructed to operate in a 100-kOe superconducting solenoid. The data indicate a Néel temperature of 58°K with large anisotropy favoring the c axis. They suggest that the antiferromagnetic structure below 58°K is an axial structure oriented along the c axis. The low-field isofields for the c axis show that at about 42°K the antiferromagnetic structure begins to square up, and at about 25°K the moments assume a ferrimagnetic structure with a net moment along the c axis at 4.2°K of $1.0 \mu_B$ per atom. The ferrimagnetic coupling can be overcome by magnetic fields above 28 kOe, yielding a ferromagnetic structure with a saturation magnetization of $7.14 \mu_B$ per atom. The b -axis sample, however, remained magnetically hard to the highest fields used; at 4.2°K the moment reached $0.75 \mu_B$ per atom at 93 kOe. The data in the paramagnetic region gave a value for μ_{eff} of $7.61 \mu_B$, with paramagnetic Curie temperatures of $\theta_{11} = 41^\circ\text{K}$, and $\theta_1 = -17^\circ\text{K}$, where θ_{11} is for fields applied along the c axis and θ_1 is for fields applied perpendicularly to the c axis.

I. INTRODUCTION

THULIUM is a trivalent hcp metal with 12 electrons in the $4f$ shell. The magnetic structure of

Tm has been determined by Koehler *et al.*¹⁻³ using neutron diffraction with both powder and single-crystal

* Work performed in the Ames Laboratory of the U. S. Atomic Energy Commission; Contribution No. 2526.

† Present address: 3M Co., St. Paul, Minn. 55119.

¹ W. C. Koehler, J. W. Cable, E. O. Wollan, and M. K. Wilkinson, *J. Appl. Phys.* **33**, 1124 (1962).

² W. C. Koehler, J. W. Cable, E. O. Wollan, and M. K. Wilkinson, *Phys. Rev.* **126**, 1672 (1962).

³ W. C. Koehler, *J. Appl. Phys.* **36**, 1078 (1965).

samples and more recently by Brun *et al.*⁴ The electrical resistivity, thermal conductivity, and thermoelectric power of single-crystal Tm samples have been reported by Edwards and Legvold.⁵ The magnetic properties of polycrystalline Tm have been measured by Rhodes *et al.*,⁶ and by Davis and Bozorth.⁷ Recently, Foner *et al.*⁸ have measured the moment of a single crystal of Tm at a temperature of 4.2°K in fields up to 140 kOe. We present here magnetization data for Tm along the $\langle 10\bar{1}0 \rangle$ (*b* axis) and $\langle 0001 \rangle$ (*c* axis) directions from 4.2 to 300°K in applied magnetic fields up to 100 kOe.

II. EXPERIMENTAL

The Tm single crystals were grown by the strain-anneal technique described by Nigh.⁹ The samples were prepared by first cutting cylinders out of a large crystal using a Servomet spark cutter. Rough spheres were cut from these cylinders by rotating them at right angles to the cylindrical cutting tool of the spark cutter. The rough spheres were trued up and polished using diamond paste and a pair of copper tools whose tips were cylinders with an inner diameter just smaller than the diameter of the sphere. The samples were then electro-polished to remove the strained material near the surface. The samples were oriented by Laue back reflection of x rays and glued to the sample holder for the magnetometer.

Calibration samples of polycrystalline high-purity Fe were prepared in a similar way from an Fe bar which had been zone refined at Battelle-Columbus for Bethlehem Steel Corp. Tables I and II give selected impurities for the Tm and Fe samples. The impurity analysis for the Fe was made at Battelle using a mass spectrometer, except where noted in the tables.

The magnetization data were taken with a vibrating-sample magnetometer designed for use in a 100-kOe

TABLE I. Selected sample impurities for Tm (ppm by weight).^a

Impurity	Concentration	Impurity	Concentration
Al	<60	Lu	<200
Ca	<20	Ho	<200
Cr	<20	Y	<200
Fe	<50	Cu	T
Mg	<10	Dy	T
Ni	<50	O ₂	83
Si	<60	N ₂	...
Er	<30	H ₂	5
Yb	<10		

^a Lanthanum, cerium, neodymium, samarium, europium, gadolinium, and terbium were not detected. N₂, O₂, and H₂ impurities were detected by vacuum-fusion analysis, and the other impurities were determined by semiquantitative analysis to an accuracy of 20%.

⁴ T. O. Brun, S. K. Sinha, and N. Wakabayashi, *Bull. Am. Phys. Soc.* **14**, 349 (1969).

⁵ L. R. Edwards and S. Legvold, *Phys. Rev.* **176**, 753 (1968).

⁶ B. L. Rhodes, S. Legvold, and F. H. Spedding, *Phys. Rev.* **109**, 1547 (1958).

⁷ D. D. Davis and R. M. Bozorth, *Phys. Rev.* **118**, 1543 (1960).

⁸ S. Foner, M. Schieber, and E. J. McNiff, Jr., *Phys. Letters* **25A**, 321 (1967).

⁹ H. E. Nigh, *J. Appl. Phys.* **34**, 3325 (1963).

TABLE II. Impurities for the Fe sample (ppm by weight).

Impurity	Concentration	Impurity	Concentration
Al	2	N ₂ (internal friction)	<0.2
As	0.4	O ₂	1.1
Ca	2	P	1.2
C (internal friction)	3.4	Pt	≤0.07
Cr	10	K	0.2
Co	10	Si	2
Cu	1.5	Ag	0.04
Ge	≤1.5	Na	0.012
H ₂	0.09	S	0.5
Mg	0.3	Ta	7
Mn	3	Sn	0.08
Hg	0.3	Ti	0.6
Mo	0.8	W	0.04
Ni	4	V	0.3
Nb	≤0.05		

superconducting solenoid. The magnetometer was patterned after the original design of Foner¹⁰ and is described elsewhere.¹¹ When taking the Fe calibration isotherms, the moment of Fe was assumed to be constant above 20 kOe, and the value used was that given by Danan.¹² This assumption was made because of the discrepancy in the published values for the high-field susceptibility.^{13,14} However, once this conflict is resolved, our data can be readily corrected for the high-field susceptibility of the Fe calibration samples.

III. RESULTS

It is appropriate to describe the neutron-diffraction results of Koehler *et al.* before presenting our magnetization data. Using powder samples, they found no long-range order above about 53°K, and at 4.2°K the effective moment per ion was found to be $(6.8 \pm 0.4)\mu_B$. From single-crystal measurements they reported a Néel temperature of 56°K with a sinusoidal antiferromagnetic structure setting in just below this temperature; i.e., the moments were found to lie along the *c* axis and their magnitude varied sinusoidally along the *c*-axis direction. As the temperature was lowered further, higher harmonics began to appear at about 40°K, which indicated the squaring up of the structure to an antiphase-domain type of structure. At 4.2°K this structure was definitely well established. This particular antiphase structure was unusual in that it was ferromagnetic with three layers of moments parallel to the *c* axis followed by four layers antiparallel to the *c* axis, giving a net moment along the *c* axis of $\sim 1.0\mu_B$.

In the more recent neutron-diffraction work on single crystals, Brun *et al.* have found that above 32°K the fundamental magnetic periodicity breaks away from

¹⁰ S. Foner, *Rev. Sci. Instr.* **30**, 548 (1959).

¹¹ D. B. Richards, Ph.D. thesis, Iowa State University, Ames, Iowa, 1968 (unpublished).

¹² H. Danan, *Compt. Rend.* **246**, 73 (1958).

¹³ A. J. Freeman, N. A. Blum, S. Foner, R. B. Frankel, and E. J. McNiff, Jr., *J. Appl. Phys.* **37**, 1338 (1966).

¹⁴ C. Herring, R. M. Bozorth, A. E. Clark, and T. R. McGuire, *J. Appl. Phys.* **37**, 1340 (1966).

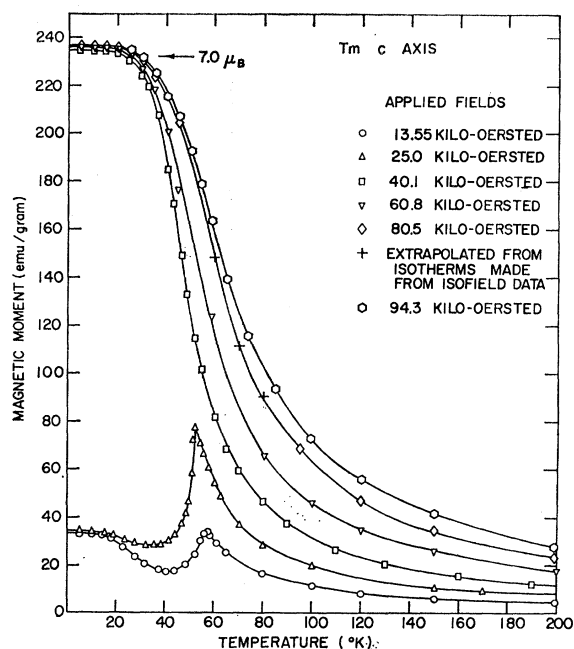


FIG. 1. Magnetic moment as a function of temperature at fixed field for the c -axis Tm crystal.

the seven-layer repeat distance previously implied to persist up to the Néel temperature by Koehler *et al.*

The low-temperature ferrimagnetic structure is shown most dramatically in the magnetization data by the isofield and isotherm data for the c axis (Figs. 1 and 2). The isofields for 13.5 and 25.0 kOe show a characteristic peak in the magnetic moment at the Néel temperature.

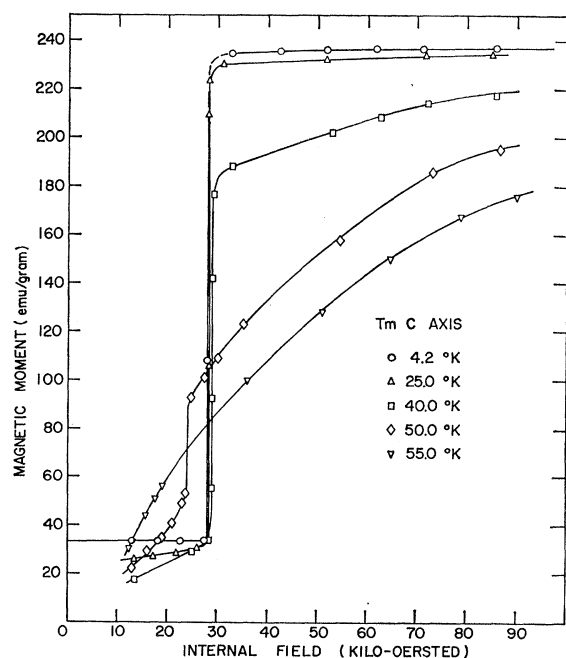


FIG. 2. Magnetic moment as a function of internal field at fixed temperature for the c -axis Tm crystal.

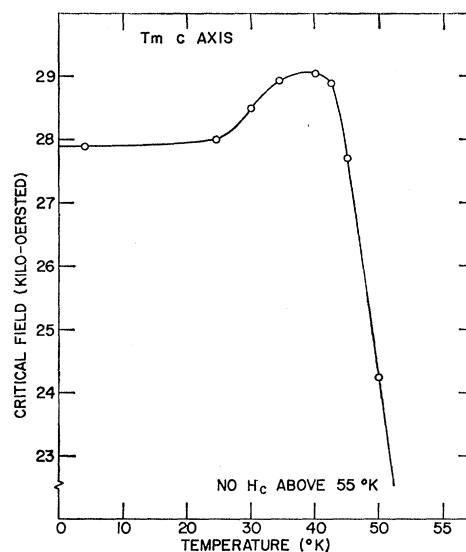


FIG. 3. Critical field as a function of temperature for the c -axis Tm crystal.

However, instead of falling smoothly to near zero, they pass through a minimum then increase to a saturation value of 33.3 and 33.5 emu/g, respectively. These saturation values are essentially constant below 10°K. Hence extrapolating linearly to zero field and averaging with the 4.2°K isotherm in Fig. 2 (this lies about 0.3% lower) gives a value of 33.25 emu/g at zero field, or a value for the moment per atom of $(1.001 \pm 0.005) \mu_B$.

The ferrimagnetic coupling can be readily overcome by a magnetic field applied along the c axis. From Figs. 1 and 2, it is apparent that nearly complete ferromagnetic alignment along the c axis can be obtained at low temperatures with internal fields just a few kilo-oersteds above some critical field. At 4.2°K the critical field is 27.9 kOe, and when the internal field is 32.7 kOe the moment has already reached $7.07 \mu_B$ per atom. By 42 kOe, Tm is essentially saturated at $7.13 \mu_B$ per atom. At 85.4 kOe it has increased to $7.14 \mu_B$ per atom, indicating a very small high-field susceptibility.

Figure 3 shows the critical field as a function of temperature. It changes very little from 4.2 to 25°K, then increases smoothly to a maximum around 39°K after which it falls off rapidly. The isotherm at 55°K showed no critical field, while the one at 50°K still indicated critical-field behavior. In Fig. 4, two 4.2°K isotherms are shown for the c -axis sample.

The isofield magnetic moments for the b -axis sample shown in Fig. 5 increase with decreasing temperature with a sharp peak near 58°K, then decrease rapidly with decreasing temperature. The temperature of the peak shifts slightly to lower temperatures with increasing applied magnetic field. This is characteristic of the transition from paramagnetism to antiferromagnetism. The Néel temperature of $58 \pm 0.5^\circ\text{K}$ found from these isofields is in good agreement with the value of 56°K .

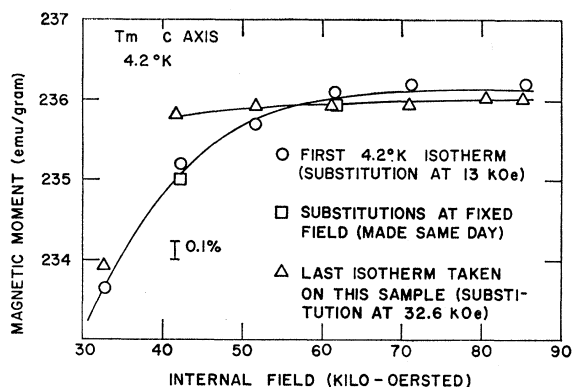


FIG. 4. 4.2°K isotherms for the *c*-axis Tm crystal.

reported by Koehler *et al.*, and the value of $57.5 \pm 0.5^\circ\text{K}$ found from electrical resistivity and thermoelectric power measurements of Edwards and Legvold.⁵

Figure 6 shows that for the *b*-axis sample Tm remains magnetically hard to at least 100 kG. The results of Foner *et al.*⁸ are in considerable disagreement with this result. It is now known that their sample, grown by vapor deposition,¹⁵ was damaged when it was pulsed to several hundred kilo-oersteds before the data were taken.¹⁶ Figure 6 indicates that in the limit of zero applied field there is no remanent moment for the *b*-axis sample.

Paramagnetic data for the *c*-axis and *b*-axis samples are shown in Figs. 7–9. The isotherms in Figs. 7 and 8

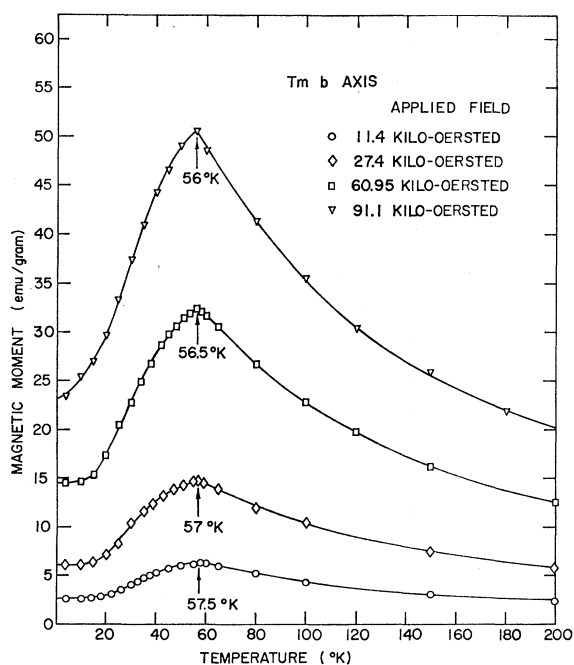


FIG. 5. Magnetic moment as a function of temperature at several fixed fields for the *b*-axis Tm crystal.

¹⁵ M. Schieber, *J. Phys. Chem. Solids Suppl.* 271 (1967).

¹⁶ S. Foner (private communication).

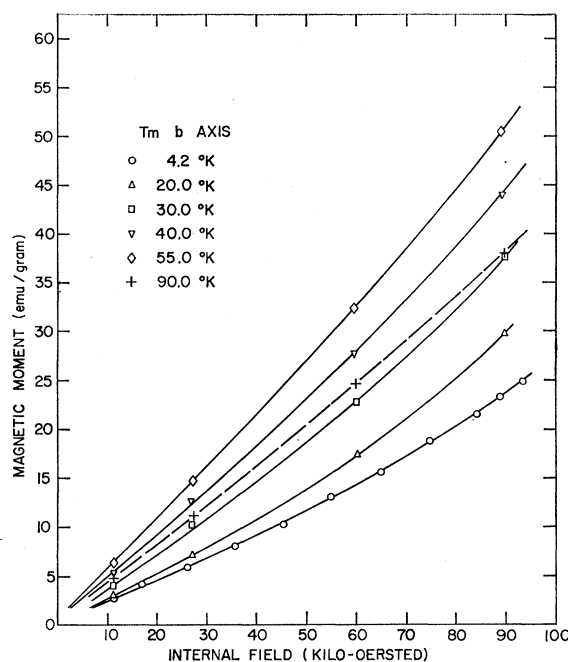


FIG. 6. Magnetic moment as a function of internal field at fixed temperature for the *b*-axis Tm crystal.

have been partially corrected for known system errors in the low-moment high-temperature region.¹¹ The plot of $1/\chi_\theta$ versus T for the *b*-axis sample (Fig. 9) gives a paramagnetic Curie temperature of -17°K , and a value for μ_{eff} , the effective moment per atom, of $7.62 \mu_B$.

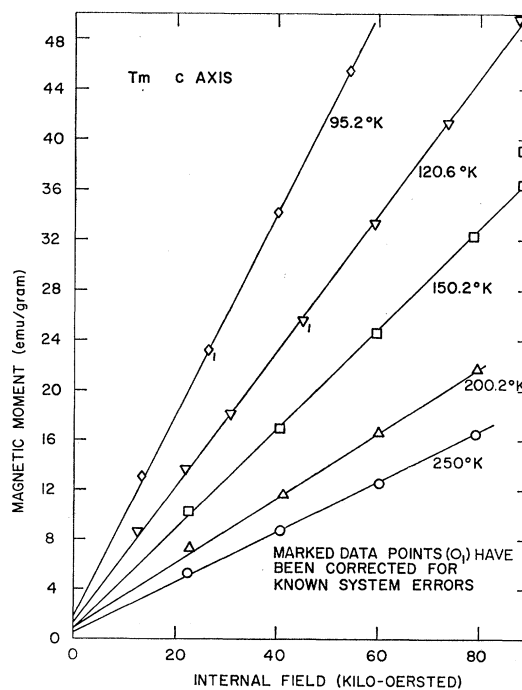


FIG. 7. Isotherms for the *c*-axis Tm crystal in the paramagnetic region.

The plot of $1/\chi_g$ versus T for the c axis gives a paramagnetic Curie temperature of 41°K, and a value for μ_{eff} of $7.61 \mu_B$. These agree well with the polycrystalline values of $7.6 \mu_B$ reported by Rhodes *et al.*,⁶ and $7.56 \mu_B$ reported by Davis and Bozorth.⁷ The theoretical value for the tripositive ion is $7.56 \mu_B$.

IV. DISCUSSION

We consider first the paramagnetic region, and use a first-order treatment; we neglect anisotropy forces but include exchange through the use of a simple Heisenberg form for the exchange Hamiltonian. Then, assuming Maxwellian statistics,

$$\sigma_g = NgJ\mu_B B_J[(gJ\mu_B/kT)(H_a + \lambda\sigma_g)], \quad (1)$$

where σ_g is the magnetization per gram, $N = N_0/A$, with N_0 being Avogadro's number and A is the atomic weight, g is the Lande factor, J is the total angular momentum, $B_J(x)$ is the Brillouin function, H_a is the applied field, and

$$\lambda = 2(g-1)^2 V/g^2 N\mu_B^2, \quad (2)$$

where V is the value for the exchange interaction summed over the entire crystal.

In the limit that the thermal energy is much greater than the magnetic energy, the magnetic susceptibility is found to be

$$\chi_g = \sigma_g/H_a = C_g/(T - \theta_C), \quad (3)$$

where $C_g = NJ(J+1)g^2\mu_B^2/3k$, and $\theta_C = \lambda C_g$.

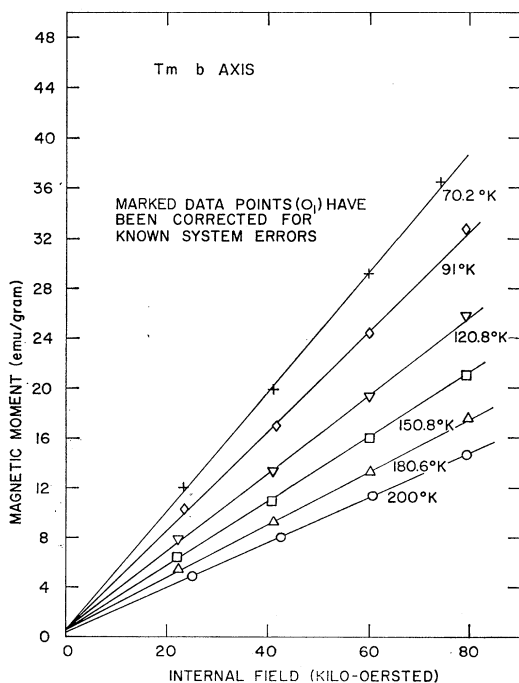


FIG. 8. Isotherms for the b -axis Tm crystal in the paramagnetic region.

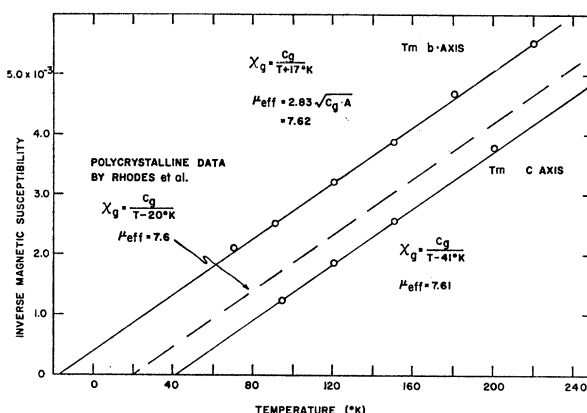


FIG. 9. Inverse susceptibility as a function of temperature for the c -axis and b -axis Tm crystals.

In the limit that $T \rightarrow 0$, and $H_a \rightarrow \infty$, Eq. (1) gives the saturation magnetization

$$\sigma_g(\infty, 0) = NgJ\mu_B, \quad (4)$$

so that the effective number of Bohr magnetons per atom is given by

$$N_{\text{eff}} = gJ. \quad (5)$$

Thulium obeys the Curie-Weiss law, Eq. (3), above the Néel temperature. The effective moment of $7.61 \mu_B$ determined in this study agrees well with that calculated for the tripositive ion of $7.56 \mu_B$ assuming Russell-Saunders coupling and Hund's rules to determine the ground state of the tripositive ion.

The expression for θ_C given in Eq. (3) is what one expects to measure for a polycrystalline sample. For single crystals the effects of anisotropy must be included. This anisotropy arises primarily from the crystalline electric field. Elliott and Stevens¹⁷ have developed an expression for the potential for the crystalline electric field for a hexagonal crystal. In this expression, the K_2^0 term is the most important. Elliott¹⁸ has shown that if K_2^0 is negative, the crystalline field anisotropy will favor alignment along the hexagonal axis. Thus the simplest form for the anisotropy energy is $K_2^0[3J_z^2 - J(J+1)]$. If this term is included with the exchange Hamiltonian, then the Curie temperatures are found to be

$$k\theta_{11} = \frac{2}{3}(g-1)^2 J(J+1)V - \frac{4}{3}K_2^0(J - \frac{1}{2})(J + \frac{3}{2}), \quad (6)$$

$$k\theta_1 = \frac{2}{3}(g-1)^2 J(J+1)V + \frac{2}{3}K_2^0(J - \frac{1}{2})(J + \frac{3}{2}),$$

where θ_{11} is the Curie temperature assuming a weak field applied parallel to the hexagonal axis, and θ_1 is the Curie temperature assuming a weak field parallel to the basal plane. It follows from Eqs. (6) that

$$k(\theta_{11} - \theta_1) = (6/5)K_2^0(J - \frac{1}{2})(J + \frac{3}{2}) \quad (7)$$

¹⁷ R. J. Elliott and K. W. H. Stevens, Proc. Roy. Soc. (London) A219, 387 (1953).

¹⁸ R. J. Elliott, in *Magnetism*, edited by G. T. Rado and H. Suhl (Academic Press Inc., New York, 1965), Vol. 2A, p. 385.

and

$$\theta_c = \frac{1}{3}(\theta_{11} + 2\theta_{12}). \quad (8)$$

Equation (8) was found *not* to hold for Tm. Both Davies *et al.*⁷ and Rhodes *et al.*⁶ found values for θ_c of 20°K using polycrystalline samples. The value of 20°K is consistent with the data for the other heavy rare earths using Eq. (3) to give the dependence of θ_c on g and J , while assuming that the value of V does not change significantly among the heavy rare earths. In this study $\theta_{11} = 41^\circ\text{K}$ and $\theta_{12} = -17^\circ\text{K}$. This would give a value for θ_c of 2°K. This difference is well outside any experimental error. Equation (8) does not hold for Tb or Dy either.^{19,20} Preferential orientation of the grains in the polycrystalline samples could explain these discrepancies.

Consider now the magnetically ordered region. The magnetization data below the Néel temperature, down to about 45°K, are consistent with the sinusoidal antiferromagnetic structure along the c axis reported by Koehler *et al.* For small applied fields, the susceptibility along the c axis is about five times larger than that along the b axis, which is consistent with large axial anisotropy. Also, the isotherms for the b -axis sample increase smoothly up to the highest field used. For a conical antiphase-domain structure there is an initial increase in magnetization (see Fig. 6) as the moments are pulled to one side of the cone. When a sufficiently high field is reached to pull moments off the cone the magnetization increases more rapidly.

The 13.55-kOe isofield for the c axis shows very succinctly the squaring up of the sinusoidal structure. The decrease in moment with decreasing temperature below the Néel temperature is typical of an antiferromagnetic structure. But at 41°K the moment goes through a minimum and begins to increase again. Thus higher harmonics are definitely present at 41°K, and probably first make a significant contribution a few degrees above this. From this isofield, it appears that the structure is essentially squared up at 20 or 25°K.

As described in Sec. III, the best value for the moment at 4.2°K and zero field is 33.25 emu/g, or $1.001 \pm 0.005 \mu_B$ atom. This agrees very well with the $-4, +3, -4, +3, \dots$ quasiantiphase domain structure along the c axis reported by Koehler *et al.*, with a moment per atom of $7.0 \mu_B$.

The plot of the critical field, H_c versus T (Fig. 3), also shows the beginning and conclusion of the squaring-up process. This can be understood by considering the expression for H_c :

$$(\langle |\mu| \rangle_7 - \langle \mu \rangle_7) H_c = F_F - F_{\text{ferri, or S. W.}}, \quad (9)$$

where $\langle \mu \rangle_7$ is the value of the magnetic moment averaged over seven layers along the c axis, $|\mu|$ is the absolute value of μ , F_F is the free energy of the ferromagnetic

¹⁹ D. E. Hegland, S. Legvold, and F. H. Spedding, Phys. Rev. **131**, 158 (1963).

²⁰ D. H. Behrendt, S. Legvold, and F. H. Spedding, Phys. Rev. **109**, 1544 (1958).

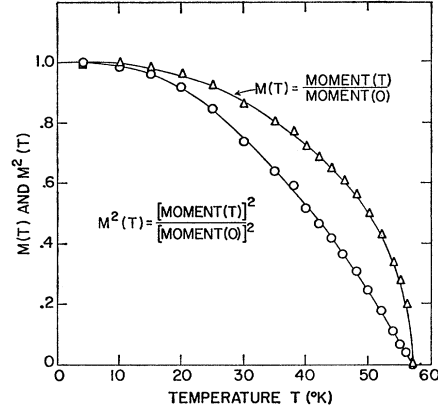


Fig. 10. Reduced moment and reduced moment per atom squared as a function of temperature for Tm(1).

structure, and F_{ferri} , or s. w. is the free energy of the ferri-magnetic or sine-wave structure, whichever is appropriate to the temperature region of interest. Equation (9) expresses the fact that the structure changes when the difference in the free energies equals the difference in the magnetic energies due to the applied field. The absolute value of μ is used in the first term on the left-hand side because, in the sinusoidal region, the applied field does not cause immediate saturation above the critical field. Instead the structure is expected to go from

$$\langle J_n^z \rangle = MJ \sin(\mathbf{q} \cdot \mathbf{R} + \delta) \quad (10)$$

to

$$\langle J_n^z \rangle \sim MJ |\sin(\mathbf{q} \cdot \mathbf{R} + \delta)|, \quad (11)$$

where \mathbf{q} is the magnetic wave vector, \mathbf{R} is a lattice vector, J is the total angular momentum quantum number, and M is the reduced moment per atom.

In the sinusoidal region $\langle \mu \rangle_7 = 0$, and $\langle |\mu| \rangle_7 = \alpha MJ$, where α is a constant whose value is near 0.7. In this region the free energies would be proportional to the reduced moment squared $M^2(T)$ (neglecting entropy). Thus, crudely, one expects the temperature dependence of H_c to be proportional to the ratio of $M^2(T)$ to $M(T)$ (functions shown in Fig. 10). Once the structure begins to square up $\langle \mu \rangle_7 \rightarrow (1/7)MJ$ and $\langle |\mu| \rangle_7 \rightarrow MJ$. Thus the left-hand side of Eq. (9) changes relatively rapidly from $\sim 0.7MJ$ to $\sim 0.85MJ$. But in this temperature region $M(T)$ is changing smoothly with temperature, and the free energies are becoming more nearly equal anyway due to the decreasing importance of the entropy contribution (i.e., $F = E - TS$). Therefore, with decreasing temperature, the rate of increase of H_c will change as the higher harmonics come in. From Fig. 3, this appears to be at about 42.5°K. Then at about 25°K, H_c becomes nearly constant. This indicates that the structure has essentially finished squaring up. The left-hand side of Eq. (9) would again be equal to a constant times MJ , while the free energies would be proportional to M^2 . But below 25°K, M and M^2 do not change

appreciably (Fig. 10), and this would leave H_c nearly constant.

The approach to saturation along the c axis for fields above the critical field was so rapid (Fig. 2) that it was not possible to determine $\sigma(\infty, 0)$ in the usual manner, i.e., plotting $\sigma(H, T)$ versus $1/H$ or $1/H^2$ to find $\sigma(\infty, T)$, then plotting $\sigma(\infty, T)$ versus $T^{3/2}$ or T^2 to obtain $\sigma(\infty, 0)$. From Fig. 1 it appears that the moment in the c -axis direction is essentially constant below 4.2°K at high fields. Hence, from an examination of Fig. 4, it was thought that Tm was essentially saturated at 60 kOe at 236.0 emu/g with a small high-field susceptibility above this. This gives a value for $\sigma(\infty, 0) \simeq \sigma(\infty, 4.2^\circ\text{K})$ of $(7.14 \pm 0.02) \mu_B$ per atom, using a value of 221.7 emu/g as the moment of Fe at 60 kOe and 4.2°K.

Figure 4 shows two 4.2°K isotherms for the c axis. The first isotherm was the first high-field low-temperature data taken on this sample. This was the first time that the ferrimagnetic structure was decoupled to give ferromagnetism. The last isotherm was taken to see if the sample had been damaged by the considerable exposure to high fields at low and moderate temperatures that it had experienced. This was done because the b -axis sample was observed to suffer permanent damage after most of the desired high-field low-temperature data had been taken. The damage was observed when an isotherm for the sample taken at 20°K showed a surprising turn upward at high fields. When the isotherm was rerun, the data showed a sharp step increase in the moment near 28-kOe internal field. (Note that this is the critical field for the c -axis direction at 20°K.) Above 28 kOe, the isotherm increased normally with field. An isotherm was then taken at 4.2°K with similarly anomalous results. It was concluded that the sample was no longer a single crystal.

The second isotherm shown in Fig. 4 was taken shortly after the solenoid had been quenched and the magnetic images were not well stabilized. The agreement between the two runs is quite good above 60 kOe. The greatest discrepancy is at 42 kOe, where the second run is about 0.3% higher. This is not really outside of experimental error, so it appears that no significant changes occurred in the c -axis sample.

The theoretical value for the saturation magnetization is $gJ = 7.0 \mu_B$. Thus the conduction electrons are contributing $(0.14 \pm 0.02) \mu_B$. The mechanism for the oscillatory exchange interaction in the heavy rare earths

is the Ruderman-Kittel-Kasuya-Yosida (RKKY) picture of indirect exchange via the polarization of the conduction electrons.²¹⁻²³ This results in a net spin polarization of the conduction electrons throughout the crystal and gives information about the density of states at the Fermi level. Because of this polarization, Liu²⁴ has shown that the conduction electrons contribute to the spontaneous magnetization of the bulk material, for a ferromagnetic structure, the amount

$$\sigma_{\theta}^e = -3ZN(g-1)V_d\mu_B J/4E_F, \quad (12)$$

where Z is the number of conduction electrons per atom, V_d is the value for the s - f exchange integral, and E_F is the Fermi energy.

We assume that the surplus moment here arises in this fashion. Since V_d and E_F change very little from Gd to Tm, σ_{θ}^e should vary as $(g-1)J$ through this series. For Gd, Nigh *et al.*²⁵ found a conduction-electron contribution of $(0.55 \pm 0.02) \mu_B$. For Gd, $(g-1)J = \frac{7}{2}$; and for Tm, $(g-1)J = 1$. This would suggest a value of $\sigma_{\theta}^e = 0.16 \mu_B$ for Tm, which agrees well with the measured value of $(0.14 \pm 0.02) \mu_B$. This, perhaps, is fortuitous because of the dependence of the surplus moment on the density of states at the Fermi level.

Including the high-field susceptibility for Fe would increase the value of $\sigma(0, \infty)$ only slightly. Using the results of Freeman *et al.*¹³ the moment of Fe at 60 kOe would be ~ 0.2 emu/g higher than at 20 kOe. This would give a value for $\sigma(0, \infty)$ of $(7.145 \pm 0.02) \mu_B$ per atom.

ACKNOWLEDGMENTS

The authors wish to thank S. H. Liu and C. A. Swenson for many informative discussions. Thanks are extended to L. Roger Edwards for growing the single crystals from which the samples used for this study were cut. The authors appreciate the cooperation of the Bethlehem Steel Corp., which supplied the pure iron for the calibrations. The authors acknowledge the interest and cooperation of F. H. Spedding in this work.

²¹ M. Ruderman and C. Kittel, *Phys. Rev.* **96**, 99 (1954).

²² P. G. deGennes, *Compt. Rend.* **247**, 1836 (1958).

²³ S. H. Liu, *Phys. Rev.* **121**, 451 (1961).

²⁴ S. H. Liu, *Phys. Rev.* **123**, 470 (1961).

²⁵ H. E. Nigh, S. Legvold, and F. H. Spedding, *Phys. Rev.* **132**, 1092 (1963).